First Photometric Analysis of the Solar-Type Binary, V428 Cep (NSV 395), in the field of NGC 188

Ronald G. Samec
Astronomy Group, Department of Natural Sciences, Emmanuel College, 181 Springs Street, Franklin Springs, GA 30639; ronaldsamec@gmail.com

Jeremy Clark
David Maloney
Astronomy Program, Department of Physics and Engineering, Bob Jones University, 1700 Wade Hampton Boulevard, Greenville, SC 29614; clarky1123@gmail.com; david.edward.maloney@gmail.com

Daniel B. Caton
Dark Sky Observatory, Physics and Astronomy Department, Appalachian State University, 525 Rivers Street, Boone, NC 28608-2106; catondb@appstate.edu

Danny R. Faulkner
Director, Johnson Observatory, 1414 Bur Oak Court, Hebron, KY 41048

Received June 25, 2016; revised September 13, October 4, 2016; accepted October 6, 2016

Abstract V428 Cep (or NSV 395) is a faint 15th magnitude binary observed in a study of the open cluster NGC 188. However, its distance from the core of the cluster might exclude its membership. Its light curve was classified as a short period EB type eclipsing binary with a period of 0.3079 d and an amplitude of ~0.7 magnitude in all curves. The difference in component temperatures is some ΔT = 180 K and its fill-out is a hefty 35%. A brief, 2.5 year period study yields, as expected, a constant period, which is 0.3076789 d. More monitoring is needed to determine its true orbital evolution. The inclination, 80º is not quite enough to produce total eclipses, so a q-search was performed using the September 17, 2004 version of the Wilson-Devinney program. Our lowest residual solution gives a q = 0.4. A cool spot was modeled on the primary component to take care of the light curve asymmetries. V428 Cep is a K-type W UMa contact binary.

1. Introduction

This paper represents the first precision, four-color, BVRI photometric study of this interesting contact binary which is in the field of the open cluster NGC 188.

2. History and observations

The variable was originally listed as short period variable NSV 395 (S8282) from photographic data (Hoffmeister 1964). It was observed in a study of the very old open cluster (age 5–7 Gyr) NGC 188 (Popov *et al.* 2013). This cluster age is what we might expect for such a W UMa binary. This paper designated it as a β Lyr-type eclipsing binary with a period of 0.3077 day and an Rmag range of 14.392–15.675 and a secondary minimum of 15.552. They gave the first published ephemeris:

$$\text{JD Hel MinI} = 2455632.260 + 0.3077\ \text{d} \times E. \qquad (1)$$

Popov *et al.*'s (2013) CCD light curves are given in Figure 1.

This system was observed as a part of our student/professional collaborative studies of interacting binaries from data taken from Dark Sky Observatory (DSO) observations. The observations were taken by Dr. Dan Caton, Dr. Ron Samec, and Jeremy Clark. Reduction and analyses were mostly done by Dr. Samec and David Maloney. Our 2013 BVRI light curves were taken with the DSO 0.81-meter reflector at Philips Gap, North Carolina, on 2, 3, and 4 November 2013 with a thermoelectrically cooled (–40ºC) 2KX2K Apogee Alta camera.

Individual observations included 128 in B and R, and 132 in V and I. The probable error of a single observation was 2% in B and V, and 1% in R and I. The relatively large errors are assumed due to the faintness of the binary. Figures 2a and 2b show sample observations of R, I, and R–I color curves on the night of 2 November, and of B, V, and B–V color curves on the night of 3 November 2013, respectively.

Our complete observations are given in Table 1, in delta magnitudes, ΔB, ΔV, ΔR_c and ΔI_c, in the sense of variable minus comparison star (V–C), phased with Equation 2.

3. Finding chart

The finding chart, given here for future observers, is shown in Figure 3. The coordinates and magnitudes of the variable star, comparison star, and check star are given in Table 2. The C–K values stayed fairly constant throughout the observing run, varying 1–2%.

4. Period study

Five times of minimum light were calculated, three primary and two secondary eclipses from our present observations:

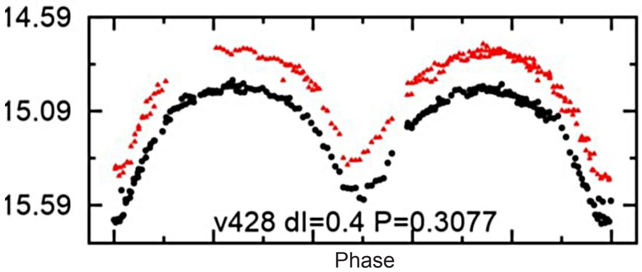

Figure 1. V428 Cep-NGC 188. R, I CCD light curves were taken by Popov *et al.* 2013.

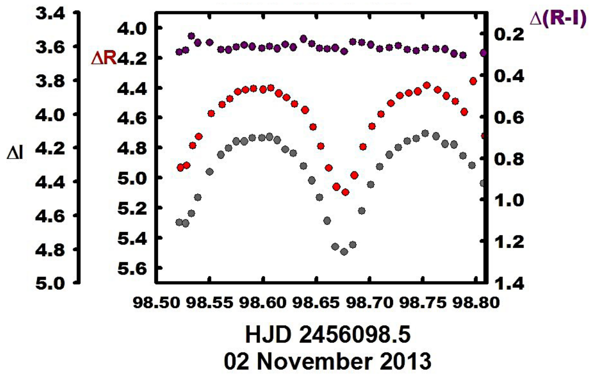

Figure 2a. V428 Cep-NGC 188. R (middle), I (bottom) delta magnitudes from sample observations and color curve (top) on 2 November 2013.

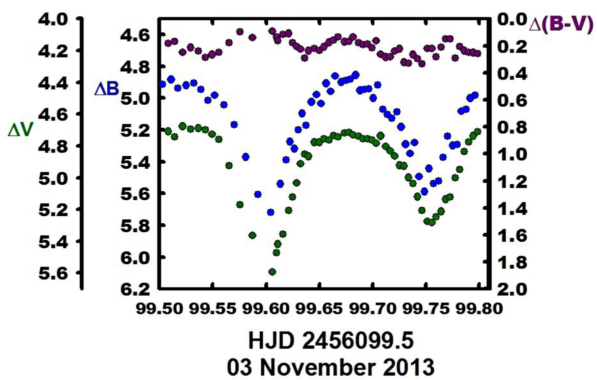

Figure 2b. V428 Cep-NGC 188. B (middle), V (bottom) delta magnitudes and color curve (top) on 3 November 2013.

HJD I = 2456598.6746 ± 0.0007
2456599.5990 ± 0.0014
2456600.8292 ±0.0013

HJD II = 2456598.8299 ± 0.0026
2456599.7549 ± 0.00025.

Six CCD times of minimum light were determined using previous observations of Popov *et al.* 2013. These were included in our determination of an improved linear ephemeris:

$$\text{HJD MinI} = 2456599.5990 + 0.30767914 \times E \quad (2)$$
$$\pm 0.0010 \quad \pm 0.00000043$$

Since this study covers only 2.5 years of observations, at least 10 more years of patrolling are needed to determine if the period is

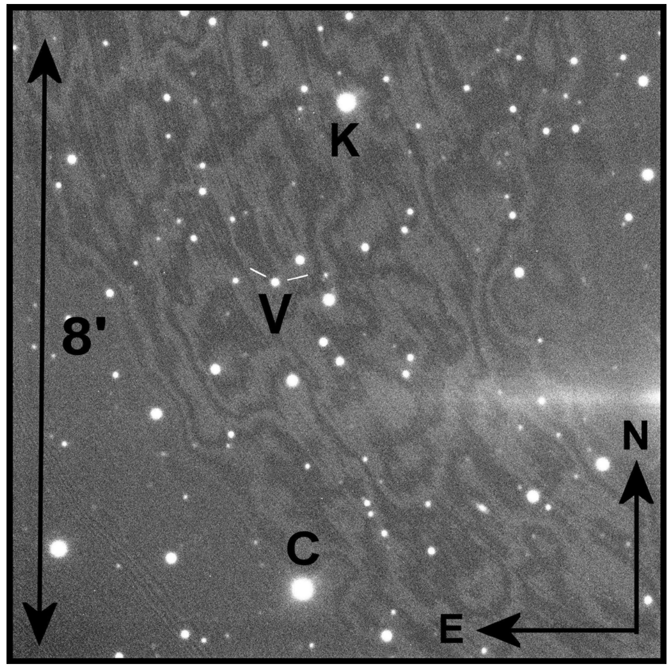

Figure 3. V428 Cep-NGC 188 finding chart. V428 Cep Variable (V), Comparison (C) and Check (K).

changing. The times of minimum light and the linear residuals are given in Table 3. Figure 4 shows the linear residuals (O–C's) from this calculation.

5. NGC 188

NGC 188 is an old open cluster of age 5–10 Gyr and has quite a few W UMa binaries (for example, six in Zhang *et al.* 2002), which fall in this age range. From his analysis of the precontact W UMa binary, V12, Meibom (2009) gives a cluster distance of 1,770 ± 75 pc and a main sequence age of 6.2 ± 0.2 Gyr. The position of V428 Cep on the color magnitude diagram is to the right of the main sequence branch before the turnoff, as expected for this cool-type binary system. We believe that the binary could well be a part of the cluster despite its position in the field (43' from the cluster center). W UMa binaries are noted for having high velocity dispersions, and it may be escaping the cluster (Guinan and Bradstreet 1988). The R, R–I color magnitude diagram is shown in Figure 5.

6. Light curve characteristics

The light curves were phased using Equation (2). These are given in Figures 6a and 6b. A table of light curve characteristics is given in Table 4. The curves are only of fair precision, averaging between 1 and 3%, probably due to the binary's faintness. The amplitude of the light curve varies from 0.76 to 0.65 magnitude in B to I, respectively. The O'Connell effect (the difference in maxima), which is classically an indication of spot activity, is slightly larger than the scatter/ averaging 4%. The difference between the two minima is substantial for a W UMa binary, some 0.1–0.2 magnitude, and is undoubtedly the reason it was designated a β Lyr type EB by Popov *et al.* (2013). However, the light curve characteristics point to a

Table 1. V428 Cep-NGC 188 observations, ΔB, ΔV, ΔR, and ΔI, variable star minus comparison star.

ΔB	HJD 2455800+	ΔB	HJD 2455800+	ΔB	HJD 2455800+	ΔB	HJD 2455800+	ΔB	HJD 2455800+
5.486	98.5258	5.029	98.7333	5.187	99.4821	5.024	99.6427	5.538	99.7570
5.404	98.5315	4.986	98.7417	5.075	99.4844	4.977	99.6475	5.523	99.7618
5.367	98.5372	4.947	98.7501	5.082	99.4906	5.036	99.6516	5.372	99.7659
5.236	98.548	4.957	98.7602	5.033	99.4929	4.908	99.6565	5.241	99.7701
5.055	98.5584	4.975	98.7686	4.905	99.4951	4.957	99.6606	5.298	99.7750
5.028	98.5658	5.044	98.777	4.913	99.4974	4.861	99.6648	5.292	99.7792
4.983	98.5731	5.055	98.7854	4.915	99.5029	4.900	99.6707	5.083	99.7833
4.928	98.5804	5.156	98.7938	4.884	99.511	4.888	99.6749	5.071	99.7876
4.941	98.5878	5.252	98.8044	4.937	99.5175	4.882	99.679	5.000	99.7917
4.901	98.5968	5.378	98.8128	4.920	99.525	4.855	99.684	4.983	99.7961
4.910	98.6041	5.527	98.8212	4.906	99.5323	4.952	99.6882	5.026	100.7737
4.922	98.6115	5.524	98.8296	4.945	99.5391	4.946	99.6924	5.011	100.7807
4.996	98.6188	5.440	98.838	5.016	99.5455	4.942	99.6965	5.050	100.7877
5.040	98.6262	5.302	98.8475	4.983	99.5519	5.000	99.7007	5.128	100.7948
5.115	98.6362	5.133	98.8559	5.043	99.5604	4.919	99.7048	5.196	100.8026
5.202	98.6436	5.025	98.8644	5.169	99.5702	5.070	99.7097	5.351	100.8097
5.279	98.6509	4.904	98.8727	5.371	99.581	5.102	99.7139	5.516	100.8171
5.335	98.6584	5.004	98.8811	5.606	99.5923	5.126	99.718	5.615	100.8241
5.518	98.6657	4.941	98.9113	5.718	99.6043	5.086	99.7227	5.673	100.8311
5.564	98.6738	4.999	98.9221	5.540	99.6136	5.182	99.7268	5.600	100.8382
5.539	98.6822	5.019	98.9302	5.390	99.6188	5.290	99.731	5.397	100.8456
5.366	98.6906	5.115	98.941	5.274	99.6226	5.350	99.7352	5.288	100.8534
5.205	98.699	5.263	98.9519	5.319	99.6265	5.281	99.7393	5.100	100.8608
5.099	98.7074	5.655	98.9599	5.201	99.6301	5.494	99.7435	5.018	100.8678
5.001	98.7165	4.989	99.4776	5.097	99.6339	5.588	99.7487		
5.064	98.7249	5.084	99.4799	5.171	99.6375	5.443	99.7528		

ΔV	HJD 2455800+	ΔV	HJD 2455800+	ΔV	HJD 2455800+	ΔV	HJD 2455800+	ΔV	HJD 2455800+
5.227	98.524	4.702	98.7388	4.946	99.479	4.778	99.650	5.137	99.769
5.173	98.530	4.679	98.7472	4.959	99.481	4.756	99.654	5.122	99.773
5.071	98.535	4.661	98.7556	4.881	99.484	4.763	99.659	5.001	99.778
5.009	98.541	4.696	98.7657	4.900	99.486	4.736	99.663	4.951	99.782
4.841	98.553	4.727	98.7741	4.790	99.492	4.744	99.668	4.838	99.786
4.790	98.563	4.764	98.7825	4.821	99.494	4.721	99.673	4.776	99.790
4.734	98.571	4.838	98.7909	4.784	99.497	4.715	99.678	4.738	99.794
4.684	98.578	4.912	98.7993	4.785	99.499	4.732	99.682	4.712	99.799
4.677	98.585	5.029	98.8099	4.710	99.509	4.740	99.687	4.708	100.759
4.653	98.593	5.149	98.8183	4.743	99.514	4.756	99.691	4.690	100.768
4.653	98.602	5.300	98.8267	4.677	99.522	4.757	99.695	4.713	100.778
4.674	98.609	5.270	98.8351	4.697	99.530	4.764	99.699	4.749	100.785
4.702	98.616	5.103	98.8435	4.690	99.536	4.784	99.703	4.826	100.792
4.760	98.624	4.972	98.853	4.701	99.543	4.738	99.708	4.906	100.799
4.759	98.631	4.864	98.8615	4.729	99.550	4.805	99.712	5.042	100.807
4.883	98.641	4.815	98.8698	4.760	99.556	4.833	99.717	5.177	100.814
4.951	98.649	4.780	98.8782	4.927	99.565	4.864	99.721	5.337	100.821
5.093	98.656	4.732	98.8866	5.172	99.576	4.924	99.725	5.362	100.828
5.247	98.663	4.683	98.8953	5.364	99.587	4.928	99.730	5.355	100.835
5.344	98.671	4.675	98.9019	5.357	99.616	5.000	99.734	5.199	100.843
5.360	98.679	4.677	98.9069	5.208	99.621	5.039	99.738	5.043	100.850
5.206	98.688	4.696	98.9164	5.124	99.625	5.121	99.742	4.894	100.858
5.028	98.696	4.749	98.9272	5.033	99.629	5.206	99.746	4.784	100.865
4.902	98.705	4.766	98.9353	4.912	99.632	5.275	99.751	4.752	100.872
4.813	98.713	4.859	98.9462	4.853	99.636	5.283	99.756		
4.739	98.722	5.062	98.957	4.867	99.640	5.248	99.760		
4.740	98.7304	5.087	98.965	4.778	99.645	5.214	99.765		

Table continued on next page

Table 1. V428 Cep-NGC 188 observations, ΔB, ΔV, ΔR, and ΔI, variable star minus comparison star, cont.

ΔR	HJD 2455800+	ΔR	HJD 2455800+	ΔR	HJD 2455800+	ΔR	HJD 2455800+	ΔR	HJD 2455800+
4.933	98.523	4.425	98.745	4.544	99.481	4.502	99.644	4.817	99.763
4.918	98.528	4.385	98.754	4.512	99.483	4.453	99.649	4.814	99.767
4.574	98.551	4.414	98.764	4.504	99.485	4.441	99.653	4.738	99.772
4.513	98.562	4.455	98.772	4.477	99.492	4.392	99.658	4.639	99.777
4.475	98.569	4.490	98.781	4.471	99.494	4.418	99.662	4.631	99.781
4.429	98.577	4.562	98.789	4.447	99.496	4.389	99.666	4.614	99.785
4.415	98.584	4.723	98.808	4.467	99.498	4.367	99.672	4.542	99.789
4.406	98.591	4.843	98.816	4.417	99.507	4.379	99.676	4.514	99.793
4.413	98.600	4.979	98.825	4.399	99.513	4.383	99.681	4.518	99.798
4.401	98.608	5.004	98.833	4.409	99.520	4.397	99.686	4.389	100.759
4.438	98.615	4.868	98.842	4.415	99.528	4.396	99.690	4.399	100.767
4.467	98.622	4.765	98.851	4.402	99.535	4.429	99.698	4.449	100.777
4.510	98.630	4.658	98.860	4.442	99.542	4.472	99.702	4.475	100.784
4.550	98.640	4.548	98.868	4.484	99.548	4.502	99.706	4.552	100.791
4.662	98.647	4.517	98.876	4.505	99.555	4.490	99.711	4.622	100.798
4.791	98.654	4.464	98.885	4.580	99.564	4.528	99.715	4.752	100.806
4.935	98.662	4.406	98.892	4.720	99.574	4.585	99.720	4.879	100.813
5.061	98.669	4.394	98.900	4.945	99.585	4.612	99.724	5.055	100.820
5.097	98.677	4.410	98.905	4.950	99.605	4.685	99.728	5.081	100.827
4.985	98.686	4.430	98.915	4.867	99.615	4.738	99.733	5.045	100.834
4.795	98.694	4.440	98.925	4.774	99.620	4.804	99.737	4.820	100.841
4.657	98.703	4.496	98.933	4.688	99.624	4.835	99.741	4.774	100.849
4.578	98.711	4.557	98.944	4.644	99.628	4.951	99.745	4.670	100.856
4.505	98.720	4.697	98.955	4.557	99.632	4.966	99.750	4.560	100.864
4.453	98.729	4.809	98.963	4.561	99.635	4.990	99.754		
4.436	98.737	4.535	99.479	4.520	99.639	4.930	99.759		

ΔI	HJD 2455800+	ΔI	HJD 2455800+	ΔI	HJD 2455800+	ΔI	HJD 2455800+	ΔI	HJD 2455800+
4.642	98.522	4.702	98.739	4.946	99.479	4.778	99.650	5.137	99.769
4.648	98.527	4.679	98.747	4.959	99.481	4.756	99.654	5.122	99.773
4.590	98.533	4.661	98.756	4.881	99.484	4.763	99.659	5.001	99.778
4.496	98.539	4.696	98.766	4.900	99.486	4.736	99.663	4.951	99.782
4.343	98.550	4.727	98.774	4.790	99.492	4.744	99.668	4.838	99.786
4.243	98.561	4.764	98.783	4.821	99.494	4.721	99.673	4.776	99.790
4.203	98.568	4.838	98.791	4.784	99.497	4.715	99.678	4.738	99.794
4.163	98.575	4.912	98.799	4.785	99.499	4.732	99.682	4.712	99.799
4.163	98.583	5.029	98.810	4.710	99.509	4.740	99.687	4.708	100.759
4.142	98.590	5.149	98.818	4.743	99.514	4.756	99.691	4.690	100.768
4.143	98.599	5.300	98.827	4.677	99.522	4.757	99.695	4.713	100.778
4.136	98.606	5.270	98.835	4.697	99.530	4.764	99.699	4.749	100.785
4.155	98.614	5.103	98.844	4.690	99.536	4.784	99.703	4.826	100.792
4.211	98.621	4.972	98.853	4.701	99.543	4.738	99.708	4.906	100.799
4.234	98.628	4.864	98.862	4.729	99.550	4.805	99.712	5.042	100.807
4.308	98.638	4.815	98.870	4.760	99.556	4.833	99.717	5.177	100.814
4.394	98.646	4.780	98.878	4.927	99.565	4.864	99.721	5.337	100.821
4.496	98.653	4.732	98.887	5.172	99.576	4.924	99.725	5.362	100.828
4.633	98.661	4.683	98.895	5.364	99.587	4.928	99.730	5.355	100.835
4.786	98.668	4.675	98.902	5.357	99.616	5.000	99.734	5.199	100.843
4.816	98.676	4.677	98.907	5.208	99.621	5.039	99.738	5.043	100.850
4.776	98.685	4.696	98.916	5.124	99.625	5.121	99.742	4.894	100.858
4.574	98.693	4.749	98.927	5.033	99.629	5.206	99.746	4.784	100.865
4.418	98.701	4.766	98.935	4.912	99.632	5.275	99.751	4.752	100.872
4.314	98.710	4.859	98.946	4.853	99.636	5.283	99.756		
4.242	98.719	5.062	98.957	4.867	99.640	5.248	99.760		
4.199	98.727	5.087	98.965	4.778	99.645	5.214	99.765		

Table 2. Information on the stars used in this study.

Star	Name	R.A. (2000) h m s	Dec. (2000) ° ′ ″	V	B–V	J–K
V	3UC350-001392[1]	01 08 12.900	+84 38 06.00	15.51	—	0.581
C	TYC 4619 738	01 07 54.577	+84 33 30.58[2]	10.917	0.535	
K (Check)	TYC 4619 618	01 07 29.1344	+84 40 41.871[2]	12.029	0.813	

[1] *USNO CCD Astrograph Catalog (Zacharias et al. 2012).* [2] *TYCHO (Perryman et al. 1997).*

Table 3. V428 Cep-NGC 188 times of minimum light and linear residuals.

No.	Epoch HJD 2400000+	Cycle	Weight	O–C	Reference
1	55632.2584	–3144.0	1.0	0.0026	Popov *et al.* 2012
2	55635.3352	–3134.0	1.0	0.0026	Popov *et al.* 2012
3	55638.2565	–3124.5	0.5	0.0009	Popov *et al.* 2012
4	55638.2593	–3124.5	0.5	0.0037	Popov *et al.* 2012
5	55639.3325	–3121.0	1.0	0.0000	Popov *et al.* 2012
6	55640.2480	–3118.0	1.0	–0.0075	Popov *et al.* 2012
7	56598.6746	–3.0	1.0	–0.0014	Present Observations
8	56598.8299	–2.5	1.0	0.0001	Present Observations
9	56599.5990	0.0	1.0	0.0000	Present Observations
10	56599.7549	0.5	1.0	0.0020	Present Observations
11	56600.8292	4.0	1.0	–0.0006	Present Observations

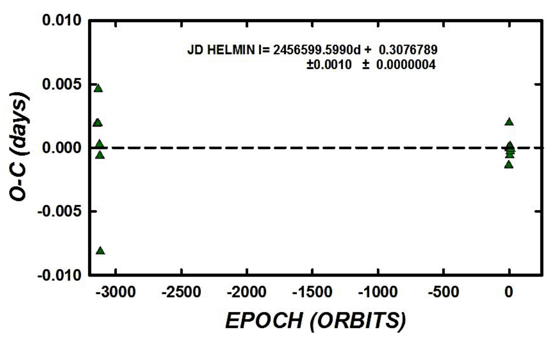

Figure 4. V428 Cep-NGC 188. Linear O–C residuals from the period study.

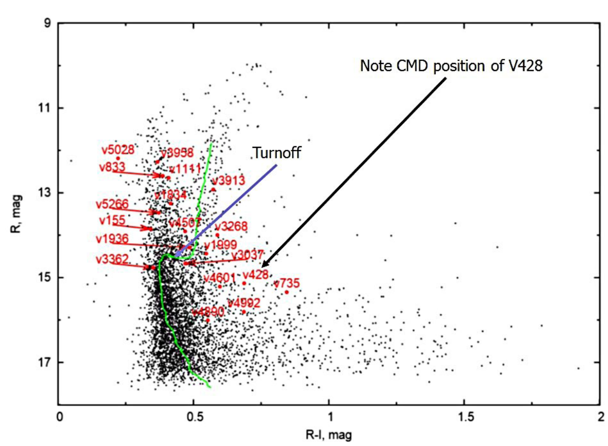

Figure 5. V428 Cep-NGC 188. R, R–I color magnitude diagram of NGC 188 with the turnoff and the position of V428 Cep identified.

contact binary—the B–V color curves dip downward at phase 0.0 and at phase 0.5, which point to each component filling its Roche Lobe. At each quadrature, beginning at phase 0.0, the Δ(B–V) values are 0.31, 0.20, 0.24, and 0.23, respectively. Thus, the curves indicate a contact, classical EW-type binary.

7. Temperature

Table 4 of Popov *et al.* (2013) gives the color indices of the newly discovered variable stars. The V428 Cep spectral type is given as K1. Its period tells us it is of class V. So we have assigned the temperature 5000 K (spectral type, K2V) to the primary component. These results closely match those of 2MASS photometry. Although its faintness is of the right magnitude and its placement is to the right of the main sequence of the CMD (Bettis 1975), its spatial position is rather far from the center of the cluster. It is assumed to be a field star (see section 4). It is of interest that K-type contact binaries, with periods shorter than 0.3 day, and the period of V428 Cep is on the borderline, are important objects for explaining the period cutoff phenomenon (Liu *et al.* 2014).

8. Synthetic light curve solution

The B, V, R, and I curves were pre-modeled with BINARY MAKER 3.0 (Bradstreet and Steelman 2002) and fits were determined in all filter bands. The resulting parameters were then averaged and input into a four-color simultaneous light curve calculation using the Wilson-Devinney Program (WD; Wilson and Devinney 1971; Wilson 1990, 1994; van Hamme and Wilson 1998). The solution was computed in Mode 3 (contact mode). Convective parameters g = 0.32, A = 0.5 were used.

Since eclipses did not appear to be quite total, a q (m_2 / m_1)-search was performed over the range q = 0.27 to 4.0 (see Figure 7). The sum of square residuals minimized at approximately q = 0.4. Beginning at this value, q was included with the rest of the adjustable parameters to obtain a final solution. The solution is given in Table 5. The normalized curves overlain by our light curve solutions are shown as Figures 8a and 8b. The geometrical (Roche-Lobe) representation of the system is given in Figures 9a, b, c, and d at the light curve quadratures so that the reader may see the placement of the spot and the relative size of the stars as compared to the orbit.

9. Discussion

V428 Cep in the field of NGC 188 is a W UMa binary in a classic contact configuration. Its spectral type, KlV, indicates

Table 4. V428 Cep-NGC 188 light curve characteristics.

Filter	*Phase*	*Magnitude Max. I*	*Phase*	*Magnitude Max. II*
	0.25		0.75	
B		4.91 ± 0.04		4.92 ± 0.03
V		4.71 ± 0.03		4.68 ± 0.03
R		4.38 ± 0.01		4.40 ± 0.01
I		4.12 ± 0.01		4.17 ± 0.02
Filter	*Phase*	*Magnitude Min. II*	*Phase*	*Magnitude Min. I*
	0.50		0.00	
B		5.51 ± 0.05		5.66 ± 0.06
V		5.27 ± 0.02		5.35 ± 0.01
R		4.96 ± 0.03		5.07 ± 0.01
I		4.67 ± 0.01		4.82 ± 0.02
Filter	*Min. I – Max. I*	*Max. I – Max. II*	*Phase*	*Min. I – Min. II*
B	0.76	0.10 ± -0.01	0.06	0.16 ± 0.11
V	0.65	0.04 ± 0.02	0.06	0.09 ± 0.03
R	0.69	0.02 ± -0.02	0.01	0.11 ± 0.04
I	0.70	0.04 ± -0.04	0.03	0.15 ± 0.03

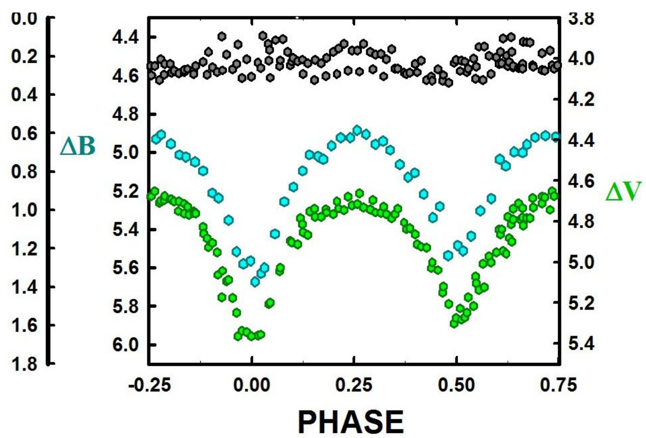

Figure 6a. V428 Cep-NGC 188. B (middle), V (bottom) delta magnitude and color magnitudes vs. phase plots in the sense of V–C (top).

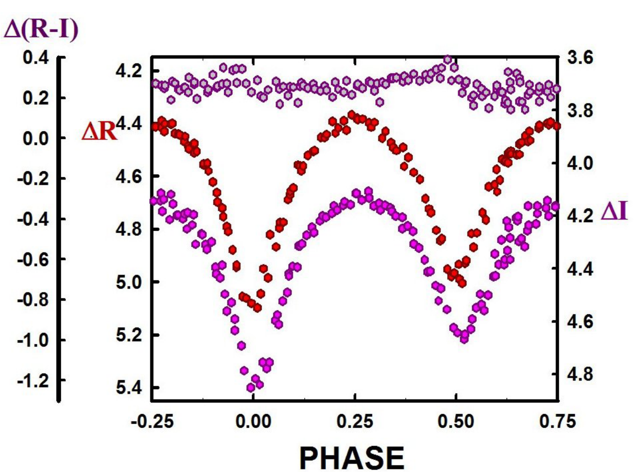

Figure 6b. V428 Cep-NGC 188. R (middle), I (bottom) delta magnitude and color magnitudes vs. phase plots in the sense of V–C (top).

Table 5. V428 Cep-NGC 188 light curve solution.

Parameters	*Values*
λ_B, λ_V, λ_R, λ_I (nm)	440, 550, 640, 790
$x_{bol1,2}$, $y_{bol1,2}$	0.643, 0. 643, 0.160, 0.160
$x_{1I,2I}$, $y_{1I,2I}$	0. 647, 0.647, 0. 183, 0. 183
$x_{1R,2R}$, $y_{1R,2R}$	0. 735, 0.735, 0. 165 0.165
$x_{1V,2V}$, $y_{1V,2V}$	0.797, 0.797, 0. 108, 0. 108
$x_{1B,2B}$, $y_{1B,2B}$	0. 852, 0.852, –0.018, –0.018
g_1 , g_2	0.32
A_1 , A_2	0.5
Inclination (°)	80.9 ± 0.1
T_1, T_2 (K)	5000, 4822 ± 6
$\Omega_1 = \Omega_2$	2. 634 ± 0.003
$q(m_2 / m_1)$	0.4228 ± 0.0009
Fill–outs: $F_1 = F_2$	34.5 ± 1.5 %
$L_1 / (L_1 + L_2)_I$	0.710 ± 0.002
$L_1 / (L_1 + L_2)_R$	0715 ± 0.002
$L_1 / (L_1 + L_2)_V$	0.724 ± 0.003
$L_1 / (L_1 + L_2)_B$	0.734 ± 0.005
JD_o (days)	2456599.6001 ± 0.0002
Period (days)	0. 30790 ± 0.00007
r_1, r_2 (pole)	0.445 ± 0.007, 0.30 ± 0.01
r_1, r_2 (side)	0.48 ± 0.01, 0.32 ± 0.01
r_1, r_2 (back)	0.51 ± 0.01, 0.37 ± 0.03
SPOT Parameters	
Spot 1 On STAR 1	*Cool Spot*
Colatitude (°)	75.0 ± 2
Longitude (°)	39 ± 1
Spot radius (°)	16.6 ± 0.5
Spot T–factor	0.89 ± 0.01
$Sum(res)^2$	0.125

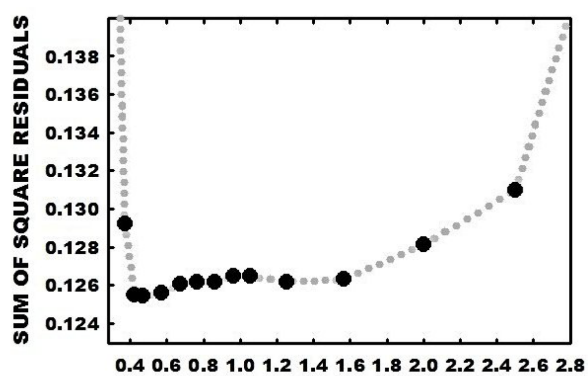

Figure 7. V428 Cep-NGC 188. Chart of solution residuals of mass ratios extending from 0.35 to 3 minimizes near 0.4.

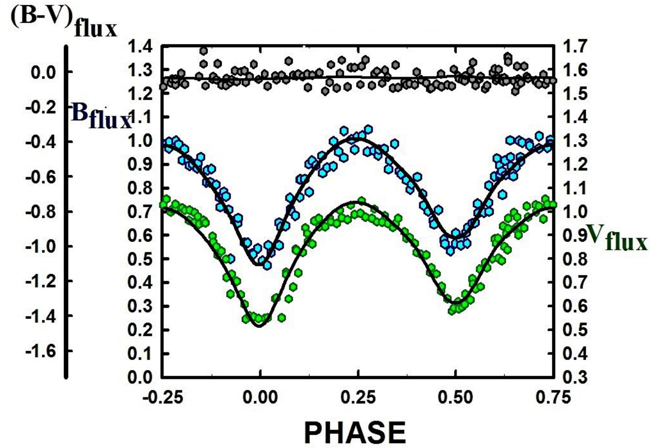

Figure 8a. V428 Cep-NGC 188. B (middle), V (bottom) synthetic light curve solutions overlaying the normalized flux curves.

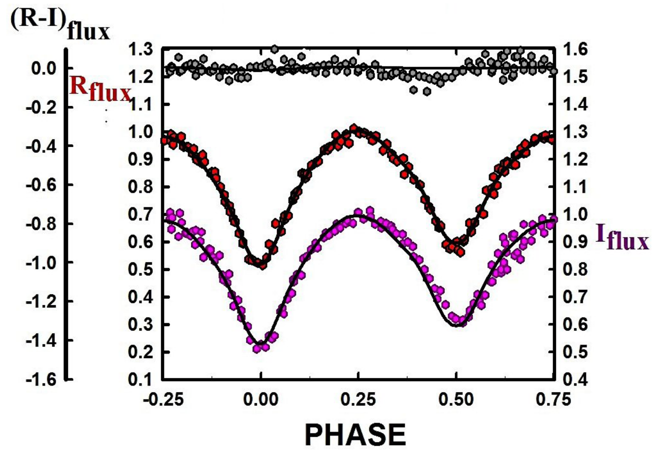

Figure 8b. V428 Cep-NGC 188. R (middle), I (bottom) synthetic light curve solutions overlaying the normalized flux curves.

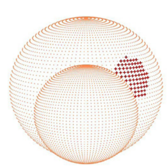

Figure 9a. V428 Cep-NGC 188. Roche Lobe surfaces from our BVRI simultaneous solution, phase 0.00 (the primary eclipse).

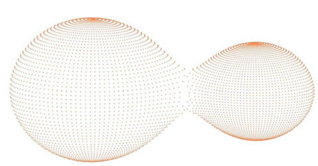

Figure 9b. V428 Cep-NGC 188. Roche Lobe surfaces from our BVRI simultaneous solution, phase 0.25.

Figure 9c. V428 Cep-NGC 188. Roche Lobe surfaces from our BVRI simultaneous solution, phase 0.50.

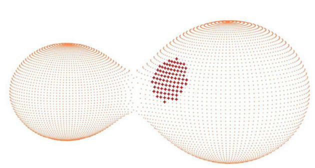

Figure 9d. V428 Cep-NGC 188. Roche Lobe surfaces from our BVRI simultaneous solution, phase 0.75.

a surface temperature of 5000 K for the primary component. The q-search indicates the mass ratio is 0.4, with a light curve amplitude of 0.76–0.65 magnitude in B to I, respectively. The secondary component has a temperature of ~4822 K (K3), which means the secondary is over luminous for its main sequence mass. The fill-out is 35%. The high inclination of 80° results in a near total eclipse with less than 1% of the light due to the secondary component at phase 0.5. It is an A-type W UMa binary that has not quite reached thermal equilibrium. The primary component was modeled with a moderately sized cool spot region of 16° radius and a mean T-factor of ~0.89 (T~4300K) -- not unusual in solar-type binaries.

10. Conclusion

Our 2.5-year period study yields little information about the orbital evolution of the binary. However, since the system has strong magnetic activity, over time, the system should slowly coalesce due to magnetic braking as it loses angular momentum due to ion winds moving outward on stiff magnetic field lines rotating with the binary (out to the Alfvén radius). If the mass ratio becomes more extreme and the fill-out increases, than we would predict the binary will coalesce, producing a rather fast rotating, single A-type main sequence field star (Guinan and Bradstreet 1988). Radial velocity curves are needed to obtain absolute (not relative) system parameters.

11. Acknowledgements

We wish to thank Bob Jones University for their coverage of travel expenses and their support of Dark Sky Observatory.

References

Bettis, C. 1975, *Publ. Astron. Soc. Pacific*, **87**, 707.

Bradstreet, D. H., and Steelman, D. P. 2002, *Bull. Amer. Astron. Soc.*, **34**, 1224.

Guinan, E. F., and Bradstreet, D. H. 1988, in *Formation and Evolution of Low Mass Stars*, ed. M. T. V. T. Lago, NATO Advanced Sci. Inst. (ASI) Ser. C, 241, Kluwer, Dordrecht, 345.

Hoffmeister, C. 1964, *Astron. Nachr.*, **288**, 49.

Liu, N.-P., Qian, S.-B., Soonthornthum, B., Leung, K.-C., Liao, W.-P., Zhu, L.-Y., He, J.-J., Liu, L., and Zhao, E.-G. 2014, *Astron. J.*, **147**, 41.

Meibom, S., *et al.* 2009, *Astron. J.*, **137**, 5086.

Perryman, M. A. C., European Space Agency Space Science Department, and the Hipparcos Science Team. 1997, *The Hipparcos and Tycho Catalogues*, ESA SP-1200 (VizieR On-line Data Catalog: I/239), ESA Publications Division, Noordwijk, The Netherlands.

Popov, A. A., Krushinsky, V. V., Avvakumova, E. A., Burdanov, A. Y., Punanova, A. F., and Zalozhnih, I. S. 2013, *Open Eur. J. Var. Stars*, **157**, 1.

van Hamme, W. V., and Wilson, R. E. 1998, *Bull. Amer. Astron. Soc.*, **30**, 1402.

Wilson, R. E. 1990, *Astrophys. J.*, **356**, 613.

Wilson, R. E. 1994, *Publ. Astron. Soc. Pacific*, **106**, 921

Wilson, R. E., and Devinney, E. J. 1971, *Astrophys. J.*, **166**, 605.

Zacharias, N., Finch, C. T., Girard, T. M., Henden, A., Bartlett, J. L., Monet, D. G., and Zacharias, M. I. 2012, *The Fourth U.S. Naval Observatory CCD Astrograph Catalog* (UCAC4), VizieR On-line Data Catalog (http://cdsarc.u-strasbg.fr/viz-bin/Cat?I/322).

Zhang, X. B., Deng, L., Tian, B., and Zhou, X. 2002, *Astron. J.*, **123**, 1548.